

## Giant Dipole Resonance - New Experimental Perspectives

Sudhee R. Banerjee\*

*Variable Energy Cyclotron Centre, 1/AF,  
Bidhan Nagar, Kolkata - 700 064, INDIA*

The study of Giant Dipole Resonance (GDR) even after more than 60 years of its discovery, still remains an intriguing and a very relevant topic of research particularly in the case of hot and fast rotating nuclei. Many new facets of this giant collective mode of vibration are being brought to light recently owing to the new age powerful detection systems. Particularly for the nuclei with large asymmetries in its neutron and protons the study of its GDR decay modes opened up very interesting research prospects worldwide. Even with low energy light-ion and heavy-ion accelerated beams and employing the powerful large volume high energy photon spectrometer LAMBDA at VECC a number of very interesting experimental observations have been made recently which radically changes the present understanding of GDR vibrations in moderately hot nuclei in general. The availability of higher energy heavy-ion beams from the near ready superconducting cyclotron at VECC will open up many more interesting and challenging research prospects with the LAMBDA spectrometer.

In recent years, great interests are being shown to understand the correct description of damping mechanisms contributing to the Giant Dipole Resonance (GDR) width at low temperatures. The damping of such giant collective vibration inside the nuclear medium occurs either due to escape of resonance energy by means of particle or photon emission (escape width) or due to its redistribution in other degrees of freedom within the system (spreading width). In medium and heavy nuclei, it turns out that the escape width only accounts for a small fraction and the major contribution of the large resonance width comes from the spreading width. The general trend of the resonance width, as deduced from the Lorentzian fit to the cross-section data, has been found to be smallest for the closed shell nuclei and larger for the nuclei between shells. However, it needs to be mentioned that for deformed nuclei, the width was obtained by fitting one single Lorentzian. Such fits never resulted in a systematic mass dependence of the width. Recently, an empirical formula has been derived for the spreading width by sepa-

rating the deformation induced widening from the spreading effect and requiring the integrated Lorentzian curves to fulfill the dipole sum rule. The relation has been found to hold good for the widths of the different

GDR components corresponding to the three axes of a deformed nucleus in general. The inclusion of the deformation in describing the apparent GDR width is also supported by the recent experimental and theoretical development in the description of the nuclear ground states. The GDR, built on excited state, is an important experimental tool since it couples directly to the nuclear shape and the investigation of its strength distribution gives a direct access to the nuclear deformation. Owing to this property, it has been applied to study Jacobi shape transition [1, 2] and hyper-deformation [2] in alpha cluster nuclei. This triaxiality is caused by J-driven deformation in high J and T regime and could be measured experimentally since the shapes are characterized by very large deformation ( $\beta \geq 0.6$ ). The experimental results have been substantiated with a theoretical calculation based on the thermal shape fluctuation model [TSFM] [3], which takes into account the J-driven deformation and T-driven shape fluctuation. For a triaxial non-rotating nucleus, the GDR strength function is a super-

---

\*Electronic address: [sudhee.banerjee@gmail.com](mailto:sudhee.banerjee@gmail.com),  
[srb@vecc.gov.in](mailto:srb@vecc.gov.in)

position of three Lorentzians that correspond to the vibration of the nucleus along each of the semi-axes [4]. The resonance energy corresponding to the each axis is obtained using the Hill-Wheeler parametrization  $E_k = E_0 \exp[-(\sqrt{5/4\pi})\beta \cos(\gamma - 2\pi k/3)]$  while the widths are calculated applying the power law  $\Gamma_k = \Gamma_0(E_k/E_0)^{1.6}$ . Whereas  $E_0$  refers to a spherical nucleus with mass A the relation between the  $E_k$  and the  $\Gamma_k$  can be generalized to hold for all nuclei with  $A > 70$  with only one proportionality constant. Further, at very high angular frequencies, these three GDR components split (the ones perpendicular to the spin axis) due to Coriolis effect as the GDR vibrations in a nucleus couple with its rotation when viewed from a non-rotating frame giving rise to five GDR components altogether. Finally, the GDR cross-section is calculated by taking into account the large amplitude thermal fluctuations using a Boltzmann probability  $e^{F(\beta,\gamma)/T}$  with the volume element  $\beta^4 \sin(3\gamma) d\beta d\gamma$ , where F is the free energy. However, for small deformations, experimentally it is not possible to measure the shape of the nucleus since thermal shape fluctuation smears out the associated splitting of the strength function resulting in an overall broadening of the distribution. Thus, only the apparent GDR widths are measured from the experiment using a statistical model analysis and compared with the TSFM, which also provides the apparent width of the GDR (in turn the shape of the nucleus). A systematic study of the thermal fluctuation model revealed the existence of a universal scaling law for the apparent width of the GDR for all T, J and A [5, 6]. The apparent width of the GDR, built on the excited states, has been found to increase monotonically ( $\sim T^{1/2}$ ) [7] beyond  $T > 1.5$  MeV. One should expect a gradual increase in the apparent GDR width from its ground state value ( $T = 0$  MeV) with the increase in temperature as predicted by TSFM. However, the temperature region below 1.5 MeV has rarely been investigated to verify if such a behavior is really true. In Sn and nearby nuclei ( $A \sim 120$ ), mostly investigated so far, only a single apparent GDR

width measurement exists for  $T < 1.2$  MeV which lies well below the TSFM prediction [8]. On the other hand, the phonon damping model (PDM) [9] which considers the coupling of the GDR phonon to particle-particle and hole-hole configurations as the mechanism for the increase of GDR width, without any need of T-driven shape fluctuations, attributes this suppression to thermal pairing which contributes even beyond 1 MeV. These two models clearly disagree with one another at temperatures below 1.5 MeV highlighting the importance of microscopic effects responsible for this unusual phenomenon. In order to address these issues and to test the validity of the theoretical models, a systematic comparison between experiment and theory over a range of temperature for several nuclei is required.

Experimentally, the measurement of GDR width at low temperature is very challenging due to the difficulties in achieving low excitation energy. Traditional heavy ion fusion reactions are limited to higher temperature due to the presence of Coulomb barrier in the entrance channel and are always associated with broad J distributions. Inelastic scattering has been used as an alternative approach with the advantage that the angular momentum transfer will be relatively low, but, the excitation energy windows are uncertain to about at least 10 MeV and hence, the estimated temperatures are less precise. Due to these reasons, very few and widely separated ( $\sim 0.25$  MeV) data points with large error bars are available. In the present work, alpha induced fusion reactions with precise experimental techniques have been used to investigate the low temperature region. In these reactions, the description of excitation energies from where the GDR photons decay will be more precise and the associated maximum angular momentum for  $A \sim 119$  mass region will be rather small ( $\sim 20\hbar$ ).

We present the first systematic and precise experimental study of angular momentum gated apparent GDR width in the unexplored low temperature region (0.9-1.4 MeV) for  $^{119}\text{Sb}$  using fusion reaction with alpha particles. The nuclear level density (NLD)

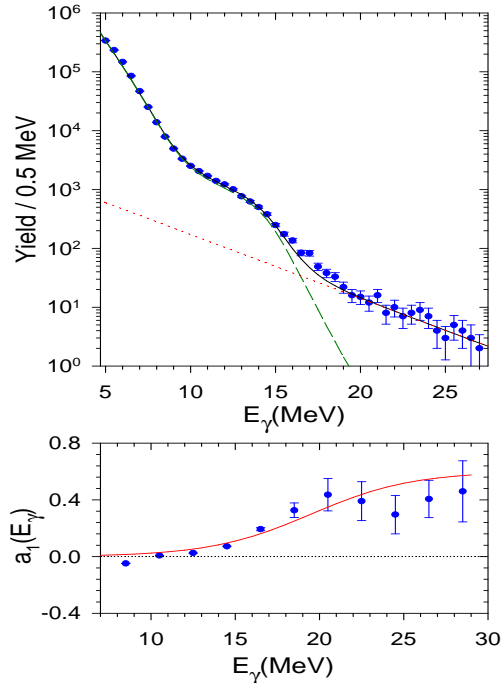


FIG. 1: (Top panel) The experimental  $\gamma$ -ray energy spectrum for  $^{119}\text{Sb}$  at 35 MeV is compared with the CASCADE prediction with the bremsstrahlung component. The individual components are also shown. (Bottom panel) The experimental  $a_1$  coefficient is compared with the exponential fit with the same  $E_0$  parameter as used for the bremsstrahlung shape.

parameter is a critical input for statistical model calculation and is also important for proper estimation of the nuclear temperature. The NLD parameter has been measured experimentally from the neutron evaporation spectrum while the bremsstrahlung contribution has been estimated using the forward/backward  $\gamma$ -ray anisotropy.

The experiment was performed at the Variable Energy Cyclotron Centre (VECC), Kolkata using accelerated alpha beams from the K-130 Cyclotron. A self-supporting 1 mg/cm<sup>2</sup> thick target of  $^{115}\text{In}$  (99% purity) was bombarded with beams of  $^4\text{He}$ . Three different beam energies of 30, 35 and 42 MeV were used to form the compound nucleus  $^{119}\text{Sb}$  at the excitation energies of 31.4, 36.2 and 43.0

MeV, respectively. The corresponding critical angular momenta were  $14\hbar$ ,  $16\hbar$  and  $18\hbar$  respectively for the three incident energies. The LAMBDA high energy photon spectrometer [10] (98 large  $\text{BaF}_2$  detectors arranged in two blocks of 7x7 each) was used to measure the high energy  $\gamma$ -rays ( $> 4$  MeV) at the angles of 55, 90 and 125 degrees with respect to the beam axis. The detector arrays were positioned at a distance of 50 cm from the target. Since, the GDR parameters depend on both the excitation energy and the angular momentum populated, it is important to separate the two effects in order to understand their individual contribution. Hence, along with the LAMBDA spectrometer, a 50-element low energy  $\gamma$ -multiplicity filter [11] was used (in coincidence with the high energy  $\gamma$ -rays) to estimate the angular momentum populated in the compound nucleus in an event-by-event mode as well as to get a fast start trigger for time-of-flight (TOF) measurements. The filter was split into two blocks of 25 detectors each which were placed on top and bottom of a specially designed scattering chamber at a distance of 5 cm from the target in a staggered castle type geometry. The TOF technique was used to discriminate the neutrons from the high energy  $\gamma$ -rays. The pulse shape discrimination (PSD) technique was adopted to reject the pile-up events in the individual detector elements by measuring the charge deposition over two integrating time intervals (30 ns and 2  $\mu\text{s}$ ) [24]. The neutron evaporation spectra were measured using seven liquid scintillator (BC501A, 5" diameter and 7" long) based neutron time of flight detectors [12] in coincidence with the multiplicity filter. The neutron detectors were placed at the angles of 30, 45, 75, 90, 105, 120 and 150 degrees with respect to the beam direction and at a distance of 150 cm from the target. The time resolution of the neutron detectors was typically about 1.2 ns which gives an energy resolution of about 15% at 1 MeV for the present setup. The GDR widths were also measured for  $^{201}\text{Tl}$  and  $^{63}\text{Cu}$ . Excited  $^{201}\text{Tl}$  and  $^{63}\text{Cu}$  compound nuclei were produced by bombarding self-supporting targets of  $^{197}\text{Au}$  and  $^{59}\text{Co}$ ,

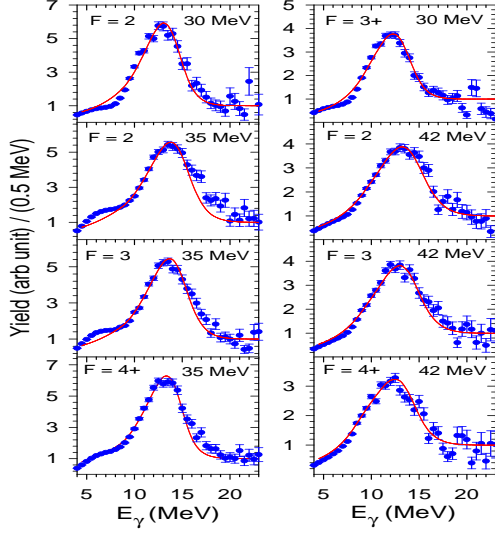


FIG. 2: Divided plots of the measured  $\gamma$ -spectra and the best fitted CASCADE calculations for different folds (F) at incident energies of 30, 35 and 42 MeV for  $^{119}\text{Sb}$ .

respectively. The initial excitation energies for  $^{201}\text{Tl}$  were 32.7, 39.6 and 47.5 MeV corresponding to incident energies of 35, 42 and 50 MeV, respectively, while it was 38.6 MeV for  $^{63}\text{Cu}$  at 35 MeV incident energy. The critical angular momenta ( $L_{cr}$ ) for  $^{201}\text{Tl}$  reactions at 35, 42 and 50 MeV incident energies were  $16\hbar$ ,  $19\hbar$  and  $22\hbar$ , respectively, while it was  $14\hbar$  for  $^{63}\text{Cu}$  at 35 MeV.

The measured high energy  $\gamma$ -ray spectra at  $90^\circ$  were compared with a modified version of the statistical model code CASCADE along with a bremsstrahlung component. The non-statistical contributions to the experimental  $\gamma$  spectra arising due to bremsstrahlung emission were parametrized using the relation  $\sigma_{brem} = k/[C + \exp(E_\gamma/E_0)]$  [13]. The center of mass  $\gamma$ -ray angular distributions were assumed to have the form  $\sigma(\theta) = A_0[1 + a_1P_1\cos(\theta) + a_2P_2\cos(\theta)]$  as the emission of  $\gamma$ -rays is dominated by electric dipole radiation. The  $a_1$  coefficient should be zero for statistical emission, however, it is nonzero for higher gamma energies due to bremsstrahlung emission. The slope parameter ( $E_0$ ) of the

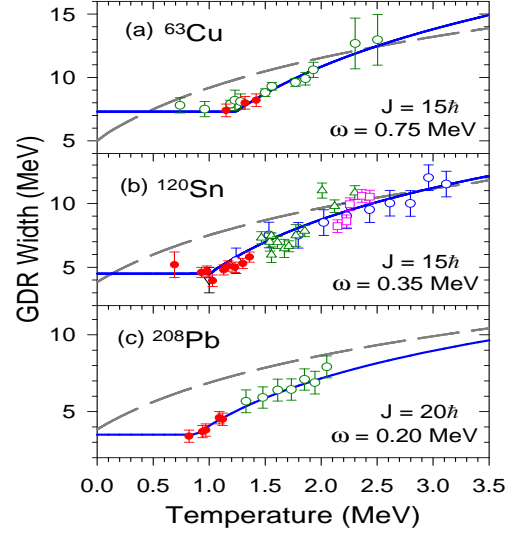


FIG. 3: The GDR widths as a function of  $T$  for  $^{63}\text{Cu}$ ,  $^{120}\text{Sn}$  and  $^{208}\text{Pb}$ . (The filled symbols are the data from the present work while open symbols are from earlier measurements. The dashed lines correspond to the pTSFM calculation while the continuous lines are the results of our CTFM (Critical Temperature included Fluctuation Model) calculation taking into consideration the effects of GDR-GQR coupling.

bremsstrahlung shape was extracted by simultaneously fitting the  $a_1$  coefficient using the exponential function with the same slope parameter. The bremsstrahlung component as well as the  $a_1$  coefficient for 35 MeV incident energy is shown in Fig. 1. The extracted value of the slope parameters are consistent with the systematics  $E_0 = 1.1[(E_{Lab} - V_c)/A_p]^{0.72}$ , where  $E_{Lab}$ ,  $V_c$  and  $A_p$  are the beam energy, Coulomb barrier and the projectile mass respectively [14].

The extracted GDR widths for all the three nuclei ( $^{63}\text{Cu}$ ,  $^{119}\text{Sb}$  and  $^{201}\text{Tl}$ ) are plotted along with the other available measurements for these systems and are shown in Fig.3. The GDR widths predicted according to the phonon damping model (PDM) [15], TSFM [16] and the phenomenological parametrization pTSFM [17] based on the TSFM as a function of  $T$  for  $^{208}\text{Pb}$  are also shown in Fig.3(c). We highlight here that the GDR

widths measured in the present work provides an important testing ground for the theoretical models at low temperature for different nuclei for which data was not available earlier. As can be seen from Fig.3, the TSFM (dashed line) fails completely to explain the experimental systematics even after incorporating the shell effects. The discrepancy, therefore, clearly indicates that the shell effect alone cannot describe the suppression of the GDR width at these low temperatures and is a general feature for all the nuclei in the entire mass range. As a matter of fact, the microscopic PDM as well, which emphasizes on the importance of the coupling of the GDR phonon to pp and hh configurations and includes the effect of thermal pairing on the GDR width, cannot explain the present measurement. Our extracted GDR widths for  $^{63}\text{Cu}$ ,  $^{201}\text{Tl}$  [19] and  $^{119}\text{Sb}$  [18] together with the previously published data for the similar systems ( $^{63}\text{Cu}$ ,  $^{120}\text{Sn}$  and  $^{208}\text{Pb}$  measured earlier) are shown in Fig.3. Interestingly, it can be seen that the GDR widths for all the three nuclei decrease with decrease in  $T$  and reach the ground state value well above  $T = 0$  MeV, which prompts us to make the assumption that the GDR vibration is not able to probe the thermal fluctuations (below  $T_c$ ) which are smaller than its own intrinsic fluctuation due to the GDR induced quadrupole moment.

Macroscopically, the isovector GDR is interpreted as the superposition of the Goldhaber-Teller (GT) and the Steinwedel-Jensen (SJ) modes where the former amounts more than the latter for all nuclei. In the SJ mode, the interpenetrating and compressible neutron and proton fluids are constrained to move within a sphere with its surface effectively clamped, which does not affect the quadrupole moment. However, the GT mode that assumes harmonic displacement of incompressible and rigid spheres of protons against neutrons induces a prolate shape with a quadrupole moment proportional to the square of the distance between the two spheres. It has been shown [20] that even though the equilibrium deformation of a nucleus increases with angular momentum, an increase of GDR width is

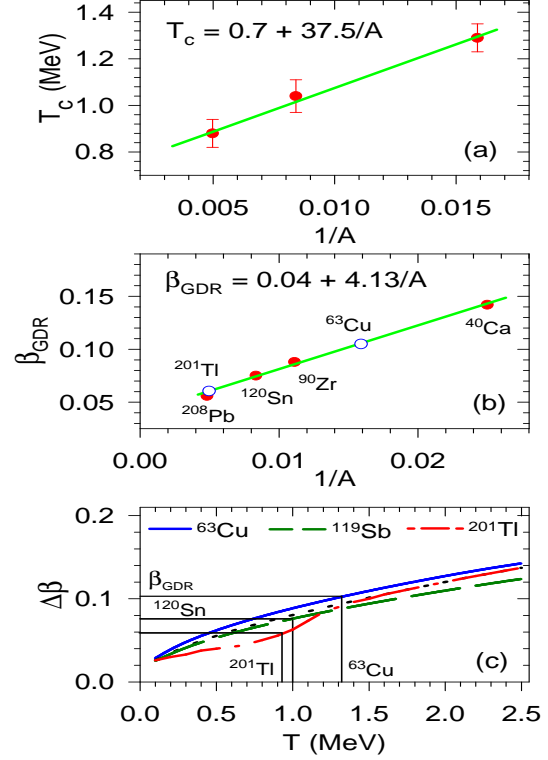


FIG. 4: (a) Critical temperature vs  $1/A$ . Experimental data (symbols) fitted with a linear function (continuous line). (b)  $\beta_{GDR}$  vs  $1/A$ . Estimated values from the quadrupole moment (filled circles) fitted with a linear function (continuous line). The  $\beta_{GDR}$  values extracted from this systematics for  $^{63}\text{Cu}$  and  $^{201}\text{Tl}$  are shown with open circles. (c) The variance of the deformation as a function of  $T$  for  $^{63}\text{Cu}$ ,  $^{119}\text{Sb}$  and  $^{201}\text{Tl}$ . The dotted line represents the calculation for  $^{201}\text{Tl}$  without including shell effect. The corresponding  $\beta_{GDR}$  is compared with  $\Delta\beta$ .

not evident experimentally until the equilibrium deformation ( $\beta_{eq}$ ) increases sufficiently to affect the thermal average. In particular, as long as  $\beta_{eq}$  is less than the variance  $\Delta\beta = [\langle \beta^2 \rangle - \langle \beta \rangle^2]^{1/2}$  the increase of GDR width is not significant. Similarly, the effect of thermal fluctuations on the experimental width should not be evident when  $\Delta\beta$  due to the thermal fluctuations is smaller than the intrinsic GDR fluctuation ( $\beta_{GDR}$ ) due to

induced quadrupole moment.

The couplings between the collective vibrations such as the isovector giant dipole and isoscalar giant quadrupole resonances have been studied in Refs. [21]. These couplings are a source of anharmonicity in the multiphonon spectrum. They also affect the dipole motion in a nucleus with static or dynamical deformation induced by a quadrupole constraint or boost, respectively. Quadrupole moment ( $Q_Q$ ) induced by the GDR motion has been calculated under the framework of time dependent Hartree-Fock theory in Refs. [21]. Using the reported values for the quadrupole moments for  $^{208}\text{Pb}$ ,  $^{120}\text{Sn}$ ,  $^{90}\text{Zr}$  and  $^{40}\text{Ca}$  as 99.0, 56.0, 46.5 and 21.4 fm<sup>2</sup>, respectively, the  $\beta_{GDR}$  values were estimated considering  $\beta \propto Q_Q / \langle r^2 \rangle$  for ellipsoidal shapes in general, where  $\langle r^L \rangle = 3R^L / (L + 3)$ . The estimated values are shown in Fig.4(b) (filled circles). It is interesting to note that the  $\beta_{GDR}$  also decreases with increase in mass and shows a linear behavior with  $1/A$  similar to the critical temperature measured in the present work. However, according to our assumption, the critical temperature should depend on the competition between  $\beta_{GDR}$  and  $\Delta\beta$ . Hence, the variance of the deformation ( $\Delta\beta$ ) for  $^{63}\text{Cu}$ ,  $^{119}\text{Sb}$  and  $^{201}\text{Tl}$  were calculated using the Boltzmann probability  $e^{F(\beta,\gamma)/T}$  with the volume element  $\beta^4 \sin(3\gamma) d\beta d\gamma$ , according to the formalism described in Ref. [22].

Thus, the competition of  $\beta_{GDR}$  and  $\Delta\beta$  giving rise to a  $T_c$  and that the experimental GDR width stays at its ground state value below  $T_c$ , clearly indicate that the GDR vibration is not able to probe the thermal fluctuations that are smaller than its own intrinsic fluctuations due to induced quadrupole moment. It has also been shown in Ref. [21] that the matrix element for the residual interaction between dipole and quadrupole vibration decreases with increase in mass number and shows a linear behavior with  $1/A$  for Sn isotopes. Interestingly, a similar behavior is observed in the present work where the critical temperature shows a  $1/A$  dependence. The appearance of a critical temperature in the variation of GDR width could perhaps be

the experimental signature of the GDR-GQR coupling at finite T. Alternatively, in order to probe this effect experimentally, one needs to examine the coupling of the  $1^-$  GDR to  $2^+$  states by measuring the decay branch of GDR to the  $2^+$  states at zero temperature. However, it will be an even more difficult experimental task to identify the GDR-GQR coupling at finite T in the statistical ensemble of states in the continuum. Hence, as it appears, the experimental GDR widths are not suppressed rather TSFM over predicts the GDR width at low temperature since it does not take into account the intrinsic GDR fluctuation induced by the GDR quadrupole moment. The experimental observation of this critical behavior in almost the entire mass range and invoking the idea of competition between the thermal and the intrinsic GDR fluctuations in explaining the critical behavior could be, in an indirect way, the experimental verification for the coupling of GDR-GQR in nuclei at finite temperatures. However, more experimental and theoretical work needs to be done.

In summary, we present the first experimental measurement of GDR width for  $^{201}\text{Tl}$ , a near Pb nucleus, in the unexplored temperature region 0.8 - 1.2 MeV and find that the extracted GDR widths are well below the prediction of TSFM even after including the shell effects. Similar results are also observed for  $^{63}\text{Cu}$  and  $^{119}\text{Sb}$ . It seems that the GDR induced quadrupole moment plays a decisive role as the GDR is not able to view the thermal fluctuations which are smaller than its own intrinsic fluctuation.

## References

- [1] A. Maj, et al., Nucl. Phys. A731 (2004) 319.
- [2] Deepak Pandit, et al., Phys. Rev. C81 (2010) 061302.
- [3] Y. Alhassid, et al., Phys. Rev. Lett. 61 (1988) 1926.
- [4] B. Bush, Y. Alhassid, Nucl. Phys. A531 (1991) 27.
- [5] D. Kusnezov, et al., Phys. Rev. Lett. 81 (1998) 542, and references therein.

- [6] Srijit Bhattacharya, et al., Phys. Rev. C78 (2008) 064601.
- [7] M. Thoennessen, Nucl. Phys. A731 (2004) 131.
- [8] P. Heckman, et al., Phys. Lett. B555 (2003) 43.
- [9] Nguyen Dinh Dang, Akito Arima, Phys. Rev. C68 (2003) 044303.
- [10] S. Mukhopadhyay, et al., Nucl. Instr. Meth. A582 (2007) 603.
- [11] Deepak Pandit, et al., Nucl. Instr. Meth. A624 (2010) 148.
- [12] K. Banerjee, et al., Nucl. Instr. Meth. A608 (2009) 440.
- [13] M.P. Kelly, et al., Phys. Rev. Lett. 82 (1998) 3404.
- [14] H. Nifenecker, J.A. Pinston, Annu. Rev. Nucl. Part. Sci. 40 (1990) 113.
- [15] Nguyen Dinh Dang, et al., Phys. Rev. Lett. 80 (1998) 4145.
- [16] W.E. Ormand, et al., Phys. Rev. Lett. 77 (1996) 607.
- [17] Dimitri Kusnezov, et al., Phys. Rev. Lett. 81 (1998) 542.
- [18] S. Mukhopadhyay, et al., Phys. Lett. B709 (2012) 9.
- [19] Deepak Pandit, et al., Phys. Lett. B713 (2012) 434.
- [20] F. Camera, et al., Nucl. Phys. A649 (1999) 115.
- [21] C. Simenel, et al., Phys. Rev. C68 (2003) 024302, and C. Simenel, et al., Phys. Rev. C80 (2009) 064309.
- [22] Deepak Pandit, et al., Phys. Rev. C81 (2010) 061302(R).